AD-A049 660 NORTH CAROLINA UNIV AT CHAPEL HILL WILLIAM R KENAN JR--ETC F/G 11/2
CHEMICALLY MODIFIED ELECTRODES. IX. X-RAY PHOTOELECTRON SPECTRO--ETC(U)
JAN 78 P R MOSES, L M WIER, J C LENNOX N00014-76-C-0817

UNCLASSIFIED TR-4 NL

| OF |
AD
A049 660

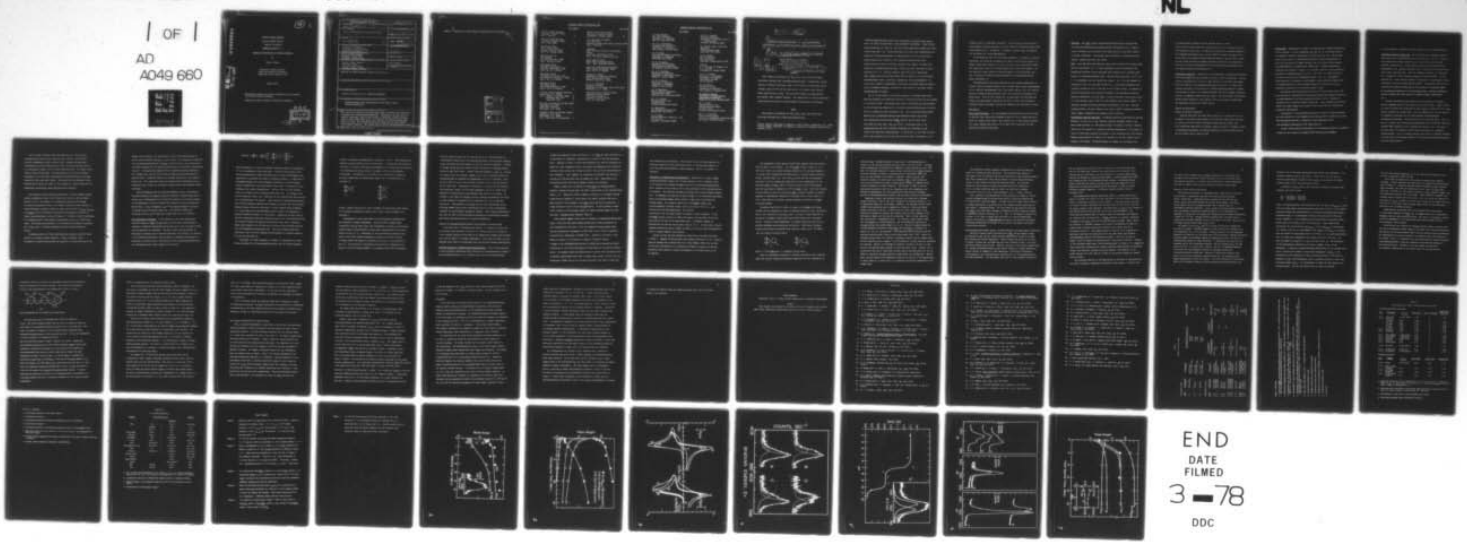

END
DATE
FILMED
3-78
DDC

(12) 2

OFFICE OF NAVAL RESEARCH

Contract N00014-76C-0817

Task No. NR 359-623

TECHNICAL REPORT NO. 4

CHEMICALLY MODIFICATION OF CARBON ELECTRODES

by

Royce W. Murray

University of North Carolina
Kenan Laboratories of Chemistry
Chapel Hill, North Carolina 27514

January 1978

SECURITY CLASSIFICATION OF THIS PAGE (When Data Entered)

REPORT DOCUMENTATION PAGE

READ INSTRUCTIONS BEFORE COMPLETING FORM

1. REPORT NUMBER: Technical Report No. 4	2. GOVT ACCESSION NO.
3. RECIPIENT'S CATALOG NUMBER	
4. TITLE (and Subtitle): Chemical Modification of Carbon Electrodes	5. TYPE OF REPORT & PERIOD COVERED: Interim
	6. PERFORMING ORG. REPORT NUMBER
7. AUTHOR(s): Royce W. Murray	8. CONTRACT OR GRANT NUMBER(s): N00014-76-C-0817
9. PERFORMING ORGANIZATION NAME AND ADDRESS: Department of Chemistry, University of North Carolina, Chapel Hill, NC 27514	10. PROGRAM ELEMENT, PROJECT, TASK AREA & WORK UNIT NUMBERS: NR 359-623
11. CONTROLLING OFFICE NAME AND ADDRESS: Office of Naval Research, Department of the Navy, Arlington, Virginia 22217	12. REPORT DATE
	13. NUMBER OF PAGES
14. MONITORING AGENCY NAME & ADDRESS (if different from Controlling Office): Office of Naval Research, ONR Branch Office, 536 South Clark Street, Chicago, Illinois 60605	15. SECURITY CLASS. (of this report): Unclassified
	15a. DECLASSIFICATION/DOWNGRADING SCHEDULE

16. DISTRIBUTION STATEMENT (of this Report)

Approved for Public Release, Distribution Unlimited

17. DISTRIBUTION STATEMENT (of the abstract entered in Block 20, if different from Report)

18. SUPPLEMENTARY NOTES

Prepared for publication in **Analytical Chemistry**

19. KEY WORDS (Continue on reverse side if necessary and identify by block number)

alkylaminisilane, ESCA, photoelectron, metal oxide, carbon, chemical modification

20. ABSTRACT (Continue on reverse side if necessary and identify by block number)

ESCA results are presented for SnO_2, RuO_2, TiO_2, and Pt/PtO oxide electrodes silanized with trialkoxyalkylaminesilanes. Observations include effects of reaction conditions, assay of the fraction of amine-like surface nitrogen, assay of N/Si surface atom ratios, O 1s spectra, and fluoride dopant depth profile in SnO_2. The silanized surfaces are amine-like but also exhibit other chemical features. The implications of various alkylaminesilane surface

over

DD FORM 1 JAN 73 1473 EDITION OF 1 NOV 65 IS OBSOLETE

SECURITY CLASSIFICATION OF THIS PAGE (When Data Entered)

BLOCK 20. structures on electrochemical applications are discussed.

TECHNICAL REPORT DISTRIBUTION LIST

	No. Copies
Office of Naval Research Arlington, Virginia 22217 Attn: Code 472	2
Office of Naval Research Arlington, Virginia 22217 Attn: Code 102IP	6
ONR Branch Office 536 S. Clark Street Chicago, Illinois 60605 Attn: Dr. George Sandoz	1
ONR Branch Office 715 Broadway New York, New York 10003 Attn: Scientific Dept.	1
ONR Branch Office 1030 East Green Street Pasadena, California 91106 Attn: Dr. R. J. Marcus	1
ONR Branch Office 760 Market Street, Rm. 447 San Francisco, California 94102 Attn: Dr. P. A. Miller	1
ONR Branch Office 495 Summer Street Boston, Massachusetts 02210 Attn: Dr. L. H. Peebles	1
Director, Naval Research Laboratory Washington, D.C. 20390 Attn: Library, Code 2029 (ONRL) Technical Info. Div. Code 6100, 6170	6 1 1
The Asst. Secretary of the Navy (R&D) Department of the Navy Room 4E736, Pentagon Washington, D.C. 20350	1
Commander, Naval Air Systems Command Department of the Navy Washington, D.C. 20360 Attn: Code 310C (H. Rosenwasser)	1
Defense Documentation Center Building 5, Cameron Station Alexandria, Virginia 22314	12
U.S. Army Research Office P.O. Box 12211 Research Triangle Park, North Carolina 27709 Attn: CRD-AA-IP	
Commander Naval Undersea Research & Development Center San Diego, California 92132 Attn: Technical Library, Code 133	1
Naval Weapons Center China Lake, California 93555 Attn: Head, Chemistry Division	1
Naval Civil Engineering Laboratory Port Hueneme, California 93041 Attn: Mr. W. S. Haynes	1
Professor O. Heinz Department of Physics & Chemistry Naval Postgraduate School Monterey, California 93940	
Dr. A. L. Slafkosky Scientific Advisor Commandant of the Marine Corps (Code RD-1) Washington, D.C. 20380	1
Advanced Research Projects Agency Materials Sciences Office 1400 Wilson Boulevard Arlington, Virginia 22209 Attn: Dr. Stan Ruby	1

TECHNICAL REPORT DISTRIBUTION LIST

	No. Copies
Dr. Paul Delahay New York University Department of Chemistry New York, New York 10003	1
Dr. R. A. Osteryoung Colorado State University Department of Chemistry Fort Collins, Colorado 80521	1
Dr. E. Yeager Case Western Reserve University Department of Chemistry Cleveland, Ohio 41106	1
Dr. D. N. Bennion University of California Energy Kinetics Department Los Angeles, California 90024	1
Dr. J. W. Kauffman Northwestern University Department of Materials Science Evanston, Illinois 60201	1
Dr. R. A. Marcus University of Illinois Department of Chemistry Urbana, Illinois 61801	1
Dr. M. Eisenberg Electrochimica Corporation 2485 Charleston Road Mountain View, California 94040	1
Dr. J. J. Auborn GTE Laboratories, Inc. 40 Sylvan Road Waltham, Massachusetts 02154	1
Dr. Adam Heller Bell Telephone Laboratories Murray Hill, New Jersey	1
Dr. T. Katan Lockheed Missiles & Space Co., Inc. P.O. Box 504 Sunnyvale, California 94088	1

	No. Copies
Dr. R. A. Huggins Stanford University Department of Materials Science & Engineering Stanford, California 94305	1
Dr. Joseph Singer, Code 302-1 NASA-Lewis 21000 Brookpark Road Cleveland, Ohio 44135	1
Dr. B. Brummer EIC Incorporated Five Lee Street Cambridge, Massachusetts 02139	1
Library P. R. Mallory and Company, Inc. P. O. Box 706 Indianapolis, Indiana 46206	1
Dr. P. J. Hendra University of Southampton Department of Chemistry Southampton S09 5NH United Kingdom	
Dr. Sam Perone Purdue University Department of Chemistry West Lafayette, Indiana 47907	1
~~Dr. Royce W. Murray~~ ~~University of North Carolina~~ ~~Department of Chemistry~~ ~~Chapel Hill, North Carolina 27514~~	1
Dr. J. Proud GTE Laboratories Inc. Waltham Research Center 40 Sylvan Road Waltham, Massachusetts 02154	1
Mr. J. F. McCartney Naval Undersea Center Sensor and Information Technology Dept. San Diego, California 92132	1

(9) Interim rept.,

(6) CHEMICALLY MODIFIED ELECTRODES. IX. X-RAY PHOTOELECTRON SPECTROSCOPY OF ALKYLAMINESILANES BOUND TO METAL OXIDE ELECTRODES

(10) P. R. Moses, Larry M. Wier[1c], John C. Lennox[2], H. O. Finklea, J. R. Lenhard, and Royce W. Murray

Kenan Laboratories of Chemistry
University of North Carolina
Chapel Hill, North Carolina 27514

(11) Jan 78

(12) 47 p.

(14) TR-4

(15) N00014-76-C-0817
NSF-MPS-75-07863

ABSTRACT

ESCA results are presented for SnO_2, RuO_2, TiO_2, and Pt/PtO oxide electrodes silanized with trialkoxyalkylaminesilanes. Observations include effects of reaction conditions, assay of the fraction of amine-like surface nitrogen, assay of N/Si surface atom ratios, O 1s spectra, and fluoride dopant depth profile in SnO_2. The silanized surfaces are amine-like but also exhibit other chemical features. The implications of various alkylamine-silane surface structures on electrochemical applications are discussed.

BRIEF

ESCA results are presented for SnO_2, RuO_2, TiO_2, and Pt/PtO oxide electrodes silanized with trialkoxyalkylaminesilanes.

[1]Present address, Department of Chemistry, Union College, Schenectady, N.Y., 12308.
[2]Present address, Department of Chemistry, University of Arkansas, Fayetteville, Arkansas, 72701.

408 860

AB

trialkoxyalkylaminesilanes react with the surfaces of several metal oxides which are useful as electrodes in electrochemical experiments. These include highly doped SnO_2 (1), RuO_2 (2), and "PtO" electrochemically formed on Pt metal (Pt/PtO electrode) (3). Carbon electrodes also react with organosilanes (4). Binding of the alkylaminesilanes to these surfaces is a first step toward immobilizing various reagents on the chemically modified electrodes. Immobilization of several reversibly reduced redox reagents via amide bond formation on alkylaminesilanized RuO_2, Pt/PtO, and SnO_2 electrodes has been described (2, 3, 5). Electron transfer reactions between immobilized redox reagents and the electrode surface may be sensitive to the connecting alkylaminesilane layer's structure, composition, and stereochemistry. We report here a number of experiments, principally using ESCA (Electron Spectroscopy for Chemical Analysis), directed at these aspects of the metal oxide/alkylaminesilane interface.

Our (1, 6) and others' (7) previous pictures of silanized metal oxide electrode surfaces were simplified versions of interfaces which are more complex in a variety of ways. The present study aims at furthering our understanding of the structure and composition of the metal oxide/alkylaminesilane interface. Parts of a model have been discussed (5, 8). The trialkoxyalkylaminesilanes employed are 3-(2-aminoethylamino)propyltrimethoxy-silane (en silane) and 3-aminopropyltriethoxysilane ($PrNH_2$ silane), and the metal oxide electrodes are SnO_2, RuO_2, TiO_2, and Pt/PtO. Continuing study of the alkylaminesilane and other silanized interfaces will doubtless in the future evoke additional understandings. In particular, we note that the four metal oxide surfaces have not been subjected with equal thoroughness to all

different types of experiments discussed. In many respects the four metal oxides appear to behave similarly, but some intrinsic differences beyond those noted probably exist. Presumption of general similarity must be regarded for the present as a crude approximation.

The observations fall into four major categories: (i) effects of reaction conditions, (ii) assay of the fraction of surface nitrogen which reacts in a normal, "amine-like" manner, (iii) assay of bound silane composition through N/Si atom ratios, and (iv) O 1s ESCA spectra of the silanized surfaces. We also describe a depth profile of fluoride dopant in SnO_2 electrodes, and a lack of success in achieving useful amidizations of alkylaminesilanized carbon electrodes (4).

Alkylaminesilanes are widely employed for the chemical modification of various silica and alumina surfaces used in bonded phase liquid chromatography (9-11), affinity chromatography (12), trace metal analysis (13, 14), immobilization of transition metal catalysts (15), and in adhesion technology (16), among others. While we have carried out few experiments on non-conducting oxides, our model appears consistent with what is known about alkylaminesilanized silica and alumina, and adds by inference some additional features.

EXPERIMENTAL

Metal Oxide Electrodes. TiO_2 was prepared in polycrystalline thin film form by chemical vapor deposition according to Bard (17) or by simply heating Ti metal in a bunsen burner flame. SnO_2 films on glass (commercially prepared) (1), spray atomized RuO_2 films on Ti (2) and Pt/PtO electrodes (3) were obtained as previously described.

Chemicals. The $PrNH_2$ silane (3-aminopropyltriethoxysilane) and en silane (3-(2-aminoethylamino)propyltrimethoxysilane) (PCR Chemical Co.), normally used as received, were for several lots vacuum distilled upon ESCA evidence of polymer contaminant. Nitrobenzoyl and fluorobenzoyl chlorides were from Aldrich. Benzene was dried over sodium.

ESCA. X-ray (Mg anode) photoelectron spectra were obtained with a DuPont 650B electron spectrometer (1). In later experiments the data acquisition and manipulation features of this instrument were modified with a microprocessor system to be described elsewhere (18). Typical vacuum level was 1×10^{-7} torr. A C 1s contaminant line was reproducibly present. B.E. of other elements are referenced to the C 1s line taken as 285.0 e.v. Sputtering experiments were typically carried out with 1.5 Kev and 35 ma Ar^+ beam current. As samples for electron spectroscopy were necessarily exposed to the atmosphere during the synthetic preparation, care was taken to avoid contaminant sources particularly of Si and nitrogen, and to check for these elements with control samples. Si remained a problem with SnO_2 electrodes as discussed in the text. Possibly excepting Pt/PtO, the metal oxides do not tend to adsorb alkylamines (probable silane reagent contaminant) from benzene control solutions.

Silanization reaction conditions. Procedures identified previously as reaction Methods A, C, and D (1, 6) are: Method A involves prolonged reflux of the metal oxide electrode in a 10% silane solution in benzene or xylene. Method C carries out the reaction in a glove box (Vacuum Atmospheres) or in syringe cap vials in 1-5% silane solutions in benzene at room temperature for 5-60 minutes. Method D uses typically 1% silane in 6°C benzene for periods ranging from 10 seconds to 10 minutes. Silanized samples are washed very thoroughly with

dry benzene before removal from the reaction flask, to avoid contact of any silane-containing solvent with atmospheric moisture, and then with methanol in many cases. An additional silanization procedure (Method E) has undergone preliminary tests; in this method the sample is reacted with silane vapor in an apparatus maintaining the sample at ca. 60°C for 12 hours. We have little ESCA data on samples prepared by Method E, but silanization does occur on RuO_2, and amidization with 3,5-dinitrobenzoyl chloride yields the expected surface electrochemistry (2).

Amidization conditions. Reaction of 3,5-dinitrobenzoyl chloride with silanized metal oxide samples has been carried out using a range of conditions. Typical solution concentration is 0.05 M in $CHCl_3$ solvent, the reaction time ranges from 10-60 minutes, and temperature from room to ca. 60°C. In some cases a catalyst base such as 2,6-lutidene or 1,8-dimethylaminonaphthalene is added, but care must be taken in the washing procedure that this nitrogen containing material is adequately washed from the sample. The latter base, for instance, adsorbs rather strongly on RuO_2 surfaces, and its use there is undesirable for experiments involving N 1s ESCA spectra.

RESULTS AND DISCUSSION

Effects of Reaction Conditions

Reaction conditions for metal oxide silanizations include the (i) pre-treatment of the metal oxide surface, (ii) conditions under which the silane is contacted with the surface and excess rinsed from the surface, and (iii) conditions under which the freshly silanized surface is handled en route to subsequent measurements or chemical reactions with the alkylamine moiety. We will discuss each of these in turn.

Pretreatment. Pretreatment is known to be important for chemical modification of SiO_2 surfaces. At room temperature only ca. 50% of the surface oxygens are thought to achieve a hydroxylated (-SiOH) state (19, 20). Except under highly acidic, basic, or dehydrating conditions, infrared measurements on TiO_2 (21), and SnO_2 (22) powders indicate that the surface lattice oxygens are predominantly in a hydroxylated (-MOH) state. Strongly dehydrating conditions are required to reduce O-H stretching intensities with generation, presumably of oxygen-bridged $M\diagup O\diagdown M$ sites. The -MOH site should constitute the reactive site for the alkoxysilane groups. Thus it is not greatly surprising that no influence of pretreatment, under conditions ranging from hot concentrated HCl to 450°C drying followed by re-exposure to air, was discerned in previous (1) and ensuing studies of SnO_2.

Pretreatment conditions employed thus far for RuO_2 and TiO_2 films have been governed by considerations of producing adherent and properly conducting or doped materials in the film preparation process itself. Exposure to laboratory air is permitted before silanization. These surfaces are reactive toward the silane reagents and we have no data suggesting that they are not extensively hydroxylated.

Pretreatment of the approximate monolayer of oxide on Pt/PtO electrodes has been restricted to low temperature oven drying (50°C) to protect the layer. The silanization reaction is sensitive to the conditions of the electrochemical preparation of the oxide layer (4).

Overall, while detailed investigation of pretreatment effects is incomplete, we have not yet, except for perhaps Pt/PtO, discerned pretreatment

to be as important a reaction condition variable as those described below.

Silanization reaction conditions. The significance of anhydrous reaction conditions for the silanization process has been emphasized (1). Growth of three-dimensional siloxane polymer can be substantially avoided under anhydrous conditions (6). Of the various reaction methods employed (see Experimental), the earliest (Method A) (1) is unnecessarily forcing for the metal oxides considered here. The room temperature Method C is convenient and is thought to yield a limiting coverage of alkylaminesilane. We have referred (6) to such limiting coverage as "monolayer" to distinguish it from "multilayer" (as with siloxane polymer growth). We emphasize that this is a reaction site-limited coverage may not be the same as a coverage limited by the molecular dimension of the alkylamine-silane. Molecular dimension-limited coverages are those typical in langmuir-Blodgett experiments (23).

The very mild Method D was originally investigated as a strategy to achieve coverages less than the reaction site-limited value. Figure 1 shows N 1s and Si 2p ESCA band intensities on SnO_2 surfaces reacted with 6°C, 1% en silane solutions for various times. The time dependence of the two elements is different; we believe the N 1s data represent alkylaminesilane coverage more accurately. The Si 2p data will be discussed later. The N 1s band is a doublet due to free base and protonated amine (N and NH^+) forms (1); relative N/NH^+ intensity is not a function of reaction time. The Figure 1 data are total N 1s intensity, which rises quite rapidly to a gradually sloping plateau. For a 3-6 minute reaction time, the N 1s intensity achieved is within 20% of the average intensity (1) for en silane reacted successfully with SnO_2 using Method A.

The N 1s data of Figure 1 show that achieving less than limiting coverages of en silane on SnO_2 using 1% silane solutions with Method D requires inconveniently short reaction times. Lowering the en silane concentration can be an effective tactic for a 30 second reaction period, as illustrated by Figure 1 for 0.1% and 0.001% solutions. The latter corresponds to about 25% coverage. The reproducibility of such low coverage experiments is not very good, and comparable experiments have not yet been conducted on the other metal oxides. Electrodes with sub-monolayer silane coverage may be useful for study of steric aspects of redox couples (2, 24) immobilized on electrodes using alkylaminesilane chemistry.

The incidence of poor electrode preparations in which siloxane polymer-forming misadventures occur is much higher with Method A than the milder Methods C and D. For example, in a comparison preparation of SnO_2/en electrodes using Methods A and D, the Method A electrode showed evidence of polymer formation by greatly reduced Sn $3d_{5/2}$ band intensity ($I_{silane}/I_{unreact}$ = 0.09 versus 0.68 on the Method D electrode) and prolonged N 1s and Si 2p signals upon sputtering, as shown in Figure 2. On Method D (and C) electrodes, N 1s disappears after a few seconds of sputtering, and Si 2p a little more slowly. Both bands were persistent on the polymer-coated Method A electrode, and Sn $3d_{5/2}$ and O 1s intensity remained low after several minutes of erosion.

We presumed earlier (1) that electrochemical properties would be quite sensitive to siloxane polymer formation. Figure 3 compares cyclic voltammetry of aqueous ferrocyanide and $Ru(bpy)_3^{2+}$ on native SnO_2 and on the

Method A and D SnO_2/en. The reversibility of both electrode reactions on native SnO_2 and Method D-SnO_2/en is quite similar. The oxidation of $Ru(bpy)_3^{2+}$ on the polymer-bearing Method A-SnO_2/en is poorly defined, very irreversible, with small currents, but the ferrocyanide reactions is only mildly irreversible (Curve C). The negatively charged $Fe(CN)_6^{4-}$ apparently readily penetrates the siloxane film, which at the solution pH employed should bear positive ammonium sites. $Ru(bpy)_3^{2+}$ tends to be excluded either due to its charge or larger size. This comparison shows that electrochemical properties are not necessarily good criteria to distinguish polymer-coated from monolayer-coated electrodes.

Gleria and Memming (25) have reported abnormally small, non-diffusion controlled currents for aqueous $Ru(bpy)_3^{2+}$ oxidation at highly doped SnO_2 in aqueous acid, interpreting this as $Ru(bpy)_3^{2+}$ adsorption on the SnO_2 surface. In our experiments, we saw no evidence for adsorption by ESCA of $Ru(bpy)_3^{2+}$-exposed SnO_2. Cyclic voltammetric $i_p/v^{1/2}$ of aqueous $Ru(bpy)_3^{2+}$ solutions is constant over 5-500 mv/sec sweep rate. The diffusion coefficient calculated from the $i_p/v^{1/2}$ data has a normal value (6×10^{-6} cm^2/sec).

Post-silanization treatment. If the reaction of the three alkoxysilane functions present on $PrNH_2$ and en silanes with the metal oxide surface is incomplete, "dangling" alkoxysilane groups may exist on the electrode surface after silanization is terminated. The fate of these dangling groups, as determined by handling of the silanized electrode, may influence the behavior of the alkylaminesilane/metal oxide interface in subsequent measurements or reactions of the amine sites. The reaction of the trialkoxyalkylaminesilane with hydroxylated metal oxide surface can be written

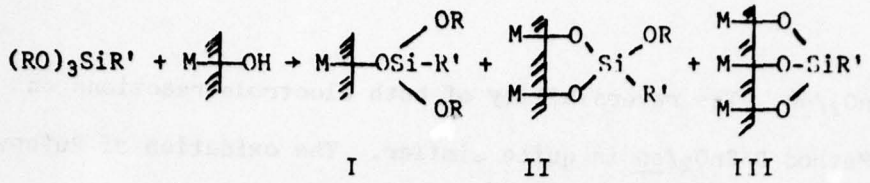

I II III

where Structures I, II, and III represent different degrees of coupling and R' is the alkylamine or some other group. Published descriptions of the relative proportions of these structures are both sparse and generally non-quantitative, as analysis for them is a difficult problem. In reactions of chloromethylsilanes with silica surfaces, Structure I is often presumed without justification other than probable bond strain in Structure III plus incomplete SiO_2 surface hydroxylation. Residual Si-Cl has been detected after silica reaction with dimethyldichlorosilane (20). An average of two Al-O-Si bonds per silane (e.g., Structure II) was reported (26) after reaction of a trichlorosilane with alumina. After reaction of dimethyldichlorosilane with tin(IV) oxide gel, Harrison and Thornton (27) showed that the silanized material reacts with acetic acid vapor to yield infrared bands assignable to a silyl ester, which was hydrolyzed slowly by water with appearance of spectral features attributed to -SiOH groups. Examination of SnO_2 films by inelastic tunneling spectroscopy following reaction with triethoxyvinylsilane has produced evidence for dangling ethoxysilane groups (28). Similarly, Raman bands assigned to Si-Cl have been observed on SnO2 following reaction with 3-chloropropyltrichlorosilane (29). Thus some evidence exists for Structures I and II and for dangling reactive groups on silanized surfaces, but none for Structure III.

Accordingly, it seems reasonable to assume in silanizations of metal oxide electrodes with trialkoxyalkylaminesilanes that the surface products

contain, or perhaps are predominantly, Structures I and II. Post-silanization handling of these surfaces can be in three modes. Assuming for the discussion Structure II, the post-silanization environment of the surface can be maintained in an anhydrous and aprotic state, to attempt to preserve the dangling alkoxysilane. Alternatively, the surface can be deliberately exposed to moisture, hydrolyzing the alkoxysilane group to an -SiOH function as in Structure IV

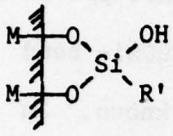

IV

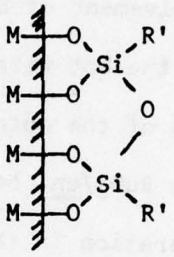

V

Thirdly, thermal curing can be used to attempt two-dimensional cross-linking of the surface, expelling H_2O and/or ROH to yield siloxane bridges as in Structure V.

Consequences of these three modes of post-silanization handling have been observed in several experiments. RuO_2 and Pt/PtO surfaces after silanization with <u>en</u> silane react with nitrobenzoyl chlorides; the resulting surfaces exhibit electrochemical surface waves characteristic of the nitro-aromatic moiety (2, 3). Differences in the electrochemical behavior were noted on the Pt/PtO surfaces depending on whether the freshly prepared Pt/PtO/<u>en</u> surface was exposed to moisture or not prior to the amidization step (3). This possibly is associated with reactivity of dangling -SiOH groups in the water-exposed samples. An analogous sensitivity of RuO_2/<u>en</u>

surfaces toward moisture was not observed (2) in the electrochemistry of nitroaromatics immobilized on the RuO_2/en electrodes, which had been thermally cured, and which were thus probably in the less reactive Structure V. Effects of thermal curing are also found in tests of stability of RuO_2/en surfaces toward hot (ca. 80°C) water. Freshly silanized RuO_2/en is stable in a variety of solvents, but a few minutes' exposure to hot water completely strips the alkylaminesilane as evidenced by disappearance of its N 1s spectrum. After curing at 85°C (in vacuo) for 30 minutes, 50-60% of the N 1s band survives the hot water test. Involvement of Structure V is implied but not proven by this experiment; whether the hot water degradation is due to -RuOSi- bond hydrolysis or dissolution of the outermost RuO_2 lattice is not known. In contrast to the result on RuO_2/en, boiling a SnO_2/en electrode for two hours in water produced no alteration in the observed N 1s or Si 2p spectral intensities. Curing effects on SnO_2/en have not been ascertained, and on Pt/PtO/en thermal curing incurs unacceptable and not further investigated increases in electrochemical background currents. These various observations show that the form of post-silanization handling is an experimental variable which merits detailed attention in electrode preparation.

Analysis of Alkylaminesilanized Metal Oxide Surfaces for Active Amine

Since one intent of alkylaminesilanization is to immobilize amine sites on the metal oxide electrode as reagents for further molecular elaboration of the surface, analysis of the fraction of immobilized nitrogen which actually will react as amine is a relevant measurement. Using ESCA N 1s data, we have measured active amine as protonatable base, and as amide-forming functionality.

Acid-Base Reactions of Immobilized Alkylaminesilane. The N 1s band observed on SnO_2 electrodes immediately after reaction with alkylaminesilane (Figure 1) and alkylpyridinesilane (1) is a doublet which from the observed binding

energies and separation (400.3 and 401.9 e.v. for $PrNH_2$ and 399.3 and 400.6 e.v. for en silane) is reasonably interpreted as a mixture of free and protonated amine. Exposure to water or dilute base diminishes but does not eliminate the higher B.E. band (unexpected since a protonated alkylammonium site attached to the metal oxide surface only through the alkyl chain should be deprotonated by this treatment). Also, exposure to strong acid (0.05 M HCl) only partially converts the free base band into the higher B.E. form. These effects are reversible and occur with little change in total N 1s intensity.

Figure 4 shows the N 1s doublet for $SnO_2/PrNH_2$ and SnO_2/en surfaces exposed to aqueous acid and base, and Table I gives areas of the resolved bands (Expts 1, 2). Taking the relative change in intensity of the higher binding energy band as a measure of active amine, the results indicate that only a small portion of the nitrogen on the $PrNH_2$ silane surface is active base. A larger fraction is active on the SnO_2/en surface. On both surfaces a significant fraction of the nitrogen retains the higher binding energy even upon base wash. RuO_2/en behaves similarly (Expt 3).

These results suggest three forms of nitrogen on alkylaminesilanized metal oxide: a form with free amine binding energy which resists protonation in acid (designated as [N] form), a form with ammonium binding energy which resists deprotonation (designated as [NH] form), and an active, reversibly protonated form (designated as [N/NH] form). Analysis of the data in this manner is subject to criticism as it neglects "transfer" effects (changes in the alkylaminesilane surface in going from an aqueous acid-base equilibrium to a dry state and thence into the vacuum of the electron spectrometer). For example, amine protonated while in contact with the aqueous acid is possibly deprotonated when dried or placed under vacuum, in which case the determined % [N/NH] form is too low and the actual % [N] form is lower than

that measured (or non-existent). The lability of the acid-base reaction is a potential liability in the active amine assay. An active amine analysis in which the amine derivatization is more permanent, such as in an amide, is desirable.

Amidization of Immobilized Alkylaminesilane. Amidization of an en or $PrNH_2$ alkylaminesilanized surface with an acid chloride or with a carboxylic acid in the presence of a dehydrating agent such as N,N'-dicyclohexylcarbodiimide (DCC), produces little change in the overall appearance of the alkylaminesilane N 1s doublet. The amide and alkylamine nitrogens have similar binding energies (31). To determine the fraction of amide nitrogen in the unresolved amine+amide band, the amidizing reagent should contain a "tag" atom with distinctive binding energy. For instance, reaction of a $SnO_2/PrNH_2$ surface with 3,5-dinitrobenzoyl chloride yields a nitro N 1s band at 406.5 e.v., well resolved from the amine+amide band. The relative intensities of the two bands reflect the extent of amide formation. If the $SnO_2/PrNH_2$ surface consists of 100% active amine, the band area of the nitro band would be 2X that of the amine+amide band. A different element can alternatively be used for the tag atom, such as F or S. In this case a relative elemental sensitivity factor becomes included in the active amine determination, which is thereby somewhat less reliable.

Results of such tag atom amidization assays for active amine are given in Table I. Examples of spectra have been reported previously (2, 3). Shake-up bands as observed for nitroanilines (32) or beam damage effects are not seen in the nitro tag spectra or in a spectrum of authentic n-propyl-3,5-dinitrobenzamide, which exhibits a stable nitro/amide N 1s band area ratio of 2/1 as expected.

The experiments on SnO_2 employ several amide reagents since the initial work was done on this material. On a SnO_2/$PrNH_2$ surface, Expts I-4, 5, 6 show only 6-27% of the surface nitrogen amidized by the indicated reagents, in contrast with SnO_2/en where 50% amidization is obtained using 3,5-dinitrobenzoyl chloride (Expt I-8). Note that en silane contains two alkylamine functions, so if one assumes that amidization occurs predominantly at the terminal primary nitrogen, Expt I-8 results indicate 100% active primary amine for en silane as compared to 6-27% for $PrNH_2$ silane. While the fraction of amine which is active on both en and $PrNH_2$ silanized surfaces is actually dependent on experimental variables as discussed below, the key result is that a lower fraction of primary nitrogen undergoes amidization on $PrNH_2$-silanized surfaces.

Incomplete reactivity of surface nitrogen on SnO_2/$PrNH_2$ and SnO_2/en surfaces can be interpreted in terms of hydrogen-bonding of amine, principally that in the γ-position on the alkyl chain, to silanol (-SiOH) functions on the parent or neighbor silane which results from hydrolysis of uncoupled silane. (In most of these experiments no special precautions were taken to maintain anhydrous post-silanization conditions.) Additionally hydrogen bonding could involve unsilanized metal hydroxyl (-MOH) sites. We suggest that the surface structures may be

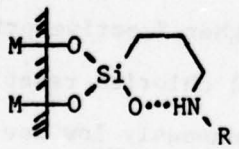

VI

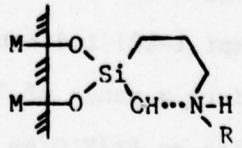

VII

where R = H for $PrNH_2$ and R = $-CH_2CH_2NH_2$ for en silane.

There is considerable precedent in previous silanization work conducted under both polymer forming and anhydrous conditions for this explanation of

inactive amine. Hydrogen bonding of amine sites in alkylaminesilanes to silanol or other surface hydroxyls has been widely inferred (33-35). Infrared spectra demonstrate the adsorption of ammonia on silanol groups at silica (36). Kahn (37) obtained evidence for liquid crystal orientations at $\underline{PrNH_2}$-silanized surfaces from which a parallel orientation of the alkylsilane chain, and hence cyclical bonding of the amine, is implied. Anderson *et al.* (38) observed a doublet N 1s ESCA band on a polymeric $\underline{PrNH_2}$ silane coating on silicon and attributed the higher binding energy nitrogen to ammonium sites caused by presence of silanol functions. The results in Table I and the postulated Structures Vi and VII are consistent with this background, and demonstrate methodology for a more quantitative description of hydrogen bonding on alkylaminesilanized surfaces than has been previously accomplished.

Depending on steric and solvation effects, the stability of hydrogen bonded Structures VI and VII may vary throughout the surface population. In an amidization assay for active amine, therefore, the unbonded "normal" amine ([N/NH] form) population may be augmented by reaction of some more weakly bonded Structures VI and VII, in which case the active amine assay is not absolute but becomes an apparent and variable quantity which depends on the amidization reagent and the reaction conditions. There is some indication that this may be a considerable effect. For instance, assay results using the 4-nitrobenzoyl, 3,5-dinitrobenzoyl, and 4-fluorobenzoyl chlorides on $SnO_2/\underline{en}$ surfaces vary widely (Expts I-7, 8, 9). The active amine assayed by 3,5-dinitrobenzoyl chloride on $RuO_2/\underline{PrNH_2}$ and $SnO_2/\underline{PrNH_2}$ is normally low (Expts 4-6, 11), but one experiment using anhydrous post-silanization and DCC coupling conditions gave a high % active amine assay (Expt I-10). Results on $RuO_2/\underline{en}$ surfaces (Expt I-12) indicate a generally higher % active primary amine but are scattered since a range of 3,5-dinitrobenzoyl chloride reaction conditions was employed. Results on Pt/PtO/*en* are probably erroneously low due to interference from adsorbed amine impurity on this particular oxide. Finally, due to interference from direct adsorption of metal ions by the SnO_2 oxide (1), we are unable to quantitate $SnO_2/\underline{en}$ reactivity toward metal ion coordination. Whether metal ions are effective in disrupting Structures VI and VII to form *en*-chelates, on these oxides or on silica (13), is a question specifically unanswered by the present data.

The amidization results generally substantiate the acid-base assay in terms of an unreactive amine population. The hydrogen bonded amines of Structures Vi and VII represent the non-protonatable [N] and non-deprotonatable [NH] forms, respectively, which should exhibit a binding energy difference similar to that between free base and protonated amine. The acid-base results for active amine are lower than those obtained by amidization so the acid-base conditions used are either less reactive at opening Structures VI and VII or do so less permanently (e.g., transfer effects).

Thus, binding of alkylaminesilane to SnO_2 and RuO_2 is thought to involve cyclical hydrogen-bonded structures whose specific reactivity depends both on silane and the assaying reagent. A larger fraction of amine can be induced to undergo amidization on *en* silane since its terminal primary amine site is less subject to hydrogen-bonding. For this reason the *en* silane is preferred over $PrNH_2$ silane when high coverages of immobilized redox couples are sought on chemically modified electrodes (2, 3). Also, in the absence of assays such as above, it is risky to assume that reactivity of a surface immobilized chemical functionality is *quantitatively* the same as its solution counterpart. Perturbing interactions not present in the solution environment can disturb a quantitative parallel.

Aklylaminesilanized Glassy Carbon: Acid-Base Behavior and Unsuccessful Amidization

Reaction of glassy carbon electrodes with $PrNH_2$ and *en* silanes in warm dry benzene for *ca.* one hour yields surfaces exhibiting N 1s and Si 2p bands more intense than typical background. These surfaces are stable to a variety of organic solvents and, provided they are first thermally cured, to hot water and dilute aqueous acid and base. However, contrary to our previous expectations (4), neither alkylaminesilanized carbon yields evidence of surface amidization using a variety of reagents at room temperature, including 4-nitrobenzoyl, 4-fluorobenzoyl, and 3-bromopropionyl chlorides and 1,1'-ferrocenedicarboxylic acid (DCC procedure). The tag element ESCA band in each attempted amidization

was not significantly different from a control (not silanized) electrode. Some loss of amine band intensity was usually noted after reaction. More forcing reaction conditions, e.g., base catalysis or elevated temperatures, resulted in cleavage of silane from the surface. Dithiocarbamate and Schiff base formations were also attempted without success. Alkylaminesilanized glassy carbon does not seem to provide useful coupling chemistry for the preparation of chemically modified carbon electrodes, at least not under monolayer coverage conditions. A different chemical approach is more successful (39).

Alkylaminesilanized glassy carbon does exhibit a protonated/free base amine N 1s doublet (4) similar to that observed on the metal oxide electrodes. Figure 5 illustrates resolution of this doublet. C/en surfaces were exposed to a series of buffer solutions, the surfaces blown dry with an air jet, and the I_{NH}/I_N intensity ratio measured. Discontinuities in I_{NH}/I_N occur (Figure 5) near the pK values (6.85 and 9.93) (40) of free ethylenediamine. The discontinuities appeared each of several times this experiment was repeated but varied as much as one pK unit. C/$PrNH_2$ surfaces, in contrast, exhibited no change in the I_{NH}/I_N ratio (0.75) over a similar pH range. These results are difficult to interpret cleanly, but could be rationalized in terms of a stable array of surface structures cyclized at the γ-amine site as in Structures VI and VII. The terminal amine of Structure VI in C/en would be more basic than that for Structure VII for the same reason that ordinary ethylenediamine exhibits two different pK values. Thus the titration of Figure 5 would correspond to neutralization of Structures VI and VII. Validity of this tentative model aside, the interesting aspect of Figure 5 is a suggestion that quantitative information on surface acid-base properties may be obtainable using a very primitive solution-to-vacuum transfer. The behavior of the buffer solution as a thin film of it dries on the surface during the transfer may be crucial.

The acid-base behavior of the C/en surface is difficult to reconcile with the lack of success in amidizing the apparent surface amine. It may be that

the loss of N 1s intensity upon attempted amidization is associated with cleavage of the active amine form of the en silane from the surface under the reaction conditions. In view of this complication, further experiments like that in Figure 5 will focus on different substrates than carbon.

Analysis of N/Si Surface Atom Ratios

The structural integrity of alkylaminesilanes immobilized on the metal oxide surface is measurable using N/Si ESCA band intensities (area). Table II gives data. Comparing surfaces prepared by reaction with en silane, I_N/I_{Si} data differ between the various metal oxides. The I_N/I_{Si} ratios tend to be low on SnO_2/en surfaces, and to depend there on silanization reaction conditions. I_N/I_{Si} values on SnO_2/en surfaces prepared under the mildest silanization conditions (Expt II-2, 10 seconds) are comparable to I_N/I_{Si} data on RuO_2/en and TiO_2/en surfaces prepared using Method C (Expts II-7, 8, 10). SnO_2/en surfaces prepared under the most forcing silanization conditions (Method A, Expt II-1) exhibit the lowest I_N/I_{Si} ratios. Pt/PtO/en surfaces exhibit high I_N/I_{Si} ratios.

The quality of the I_N/I_{Si} data is of course influenced by background N 1s and Si 2p bands. Unreacted samples of RuO_2 and TiO_2 are typically free from significant N 1s or Si 2p blanks. On SnO_2, however, a Si 2p background appears at the same B.E. as the silane band, with erratically varying intensities (entirely absent on occasional samples and amounting to 50% of the band on a silanized SnO_2 surface in other instances). A background correction was not attempted due to this inconsistent behavior, and the SnO_2/en I_N/I_{Si} are thus known to be low. It is not clear, however, that the Si background problem can account for the systematic variation of SnO_2/en surfaces with silanization reaction conditions. Relative to RuO_2/en and TiO_2/en, then, except for the mild silanization reaction condition, the SnO_2/en surfaces appear qualitatively Si-rich (or N-poor). On Pt/PtO surfaces, no difficulties exist with Si blanks as long as silicon-containing polishing materials are

avoided in the Pt electrode resurfacing which follows each experiment. N 1s background bands are seen at ca. 400 e.v. from time to time but are not typically large enough to cause as high a I_N/I_{Si} as observed on Pt/PtO/en surfaces (Expt II-11), which seem to be N-rich.

Conversion of I_N/I_{Si} data to N/Si atom ratios involves a relative ESCA elemental sensitivity factor

$$\frac{I_N}{I_{Si}} = \left[\frac{\sigma_N \lambda_N \phi_N}{\sigma_{Si}\lambda_{Si}\phi_{Si}}\right] \frac{T_N C_N D_N}{T_{Si}C_{Si}D_{Si}} \qquad (1)$$

where σ is photoionization cross-section for the N 1s and Si $2p_{(1/2+3/2)}$ levels, λ are the escape depths for photoelectrons from these levels, ϕ is the angular correlation factor for photoelectrons at the photon beam-sample-spectrometer acceptance angle, T is spectrometer efficiency for electrons of the given kinetic energies, C is an attenuation factor for adsorbed contaminant hydrocarbon layer on the sample, and D is atom density. Using computed and tabularized (30) cross-sections $\sigma_N/\sigma_{Si(2p)} = 2.06$; $\phi_N/\phi_{Si(2p)}$ is calculable (41) (equals 1.107 for our spectrometer's 67° angle); and λ_N/λ_{Si} is estimable from the $\lambda\alpha(KE)^{0.75}$ relationship which at KE ≥ 300 e.v. is a good approximation (42) to a more exact formulation (43) (equals 0.80 for N 1s/Si 2p). The term in brackets in equation 1 is thus 1.82 for N 1s/Si 2p. The dispersion of our spectrometer's efficiency with kinetic energy, if any, is not documented. It employs a voltage retarding feature which at the extreme could yield a relation (44) $T\alpha(KE)^{-1}$, which would correspond to $T_N/T_{Si} = 1.35$. Attenuation by the contaminant is also an uncertain factor; if the film is assumed to be ca. 20 Å hydrocarbon, which is probably generous, a very rough calculation gives $C_N/C_{Si} \sim 0.8$ (attenuation is larger for the lower KE N 1s photoelectrons). The last two factors tend to cancel one another,

and if we then assume $T_N C_N / T_{Si} C_{Si} \sim 1.0$, the theoretical estimate for the N 1s/Si 2p sensitivity ratio is 1.82.

The N 1s/Si 2p sensitivity ratio was also evaluated with chemical standards. Several materials (not sputtered) are compared to the theoretical value in Table II. Prepared, analyzed (bulk) alkylamine siloxane polymers agree reasonably well with the theoretical value. Data for Si_3N_4 agree less well. Previous (45, 46) sputter profiles of Si_3N_4, however, suggest that its unsputtered surfaces tend to be N-poor. Other available standards work likewise notes a problem with Si data (42). The 1.82 factor was adopted for conversion of I_N/I_{Si} in Table II to N/Si atom ratios, but the reader will note that use of a 1.31 factor from the Si_3N_4 sample would not alter essential features of the following discussion.

Examining RuO_2 electrodes first, the calculated N/Si atom ratios on electrodes silanized with $\underline{PrNH_2}$, en, and triam silanes are in reasonable agreement with the ideal molecular ratios. The result for TiO_2/en is similar. Structural degradation of the alkylaminesilane does not appear to occur upon binding to these surfaces.

The N/Si atom ratio results for SnO_2/en surfaces, known to involve error from the Si background problem, suggest a non-ideal N/Si surface stoichiometry, particularly for surfaces prepared under the more vigorous reaction conditions. Two explanations for silicon-richness on a silanized metal oxide surface can be offered. First, it is possible that the silane reagents contain deaminated trialkoxyalkylsilanes or these are produced by decomposition pathways in the reacting solution. Secondly, the silane reagent may penetrate the outermost, hydrated one or two atomic layers of the SnO_2 lattice,

nucleophilic attack by -SnOH on the alkylamine sidechain then occurring to expel that group with its amine nitrogen. The silicon would reside as silicate sites interspersed in the surface SnO_2 lattice, as below

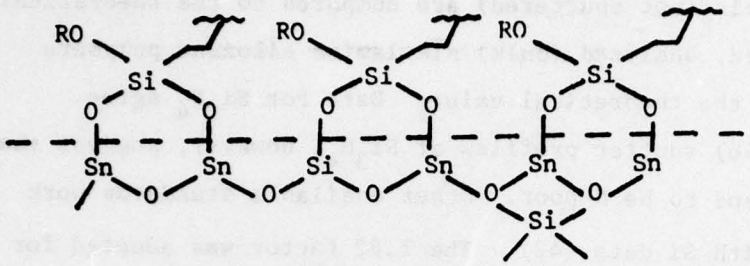

VIII

Both explanations for Si-richness are speculations.

The N/Si atom ratio on Pt/PtO/<u>en</u> shows that this surface is N-rich. The Pt/PtO surface differs from the other electrodes in that the oxide layer is an approximate monolayer rather than a bulk oxide (3). This oxide, or patches of exposed Pt^o, may chemisorb amine components from decomposed alkylaminesilane in the reacting solution. If so, the amine+amide N 1s band of Table I is enhanced on Pt/PtO and the active amine assay of Table I (Expts I-14, 15) is thereby low. Electrochemical experience with the Pt/PtO/en surface suggests fairly high coverages in amidization reactions (3), and the portion of immobilized alkylaminesilane which reacts as active amine may be higher than that represented in Table I by 2X or more. If, for instance, we assume the reactivity of <u>en</u> silane on Pt/PtO/<u>en</u> is like that on SnO_2/<u>en</u> surfaces (e.g., 50% active amine), and then employ I_N/I_{Si} data taken using the 406 e.v. nitro band on a silanized, amidized electrode (Expt II-12), an atom ratio more in line with the results on RuO_2/<u>en</u> and TiO_2/<u>en</u> surfaces results. A better-substantiated quantitative picture of the alkylaminesilane stoichiometry on Pt/PtO/<u>en</u> surfaces than this is obviously desirable but will require further experiments.

Effect of Silanization on O 1s Spectra of Metal Oxides

Each of the three bulk metal oxide electrodes exhibits a dominant O 1s band which is presumably the lattice -MOM- oxygen, and also a higher B.E. O 1s band which is poorly resolved from the main band for SnO_2 (Figure 6, Curve D) but distinct for RuO_2 and TiO_2 (Curves A, F). The SnO_2 shoulder has been observed by others (7, 47), and similar shoulders are common observations (48-54) on other metal oxides especially upon exposure to air and moisture. A collection of metal oxide O 1s data is given in Table III. The higher B.E. shoulder is usually interpreted as surface hydroxyl (7, 47, 50-54) although evidence for a different metal oxidation state was presented for RuO_2 (48).

Reaction of the metal oxide electrodes with an organosilane produces a much more prominent higher B.E. O 1s band (Curves B, C, E, G, Figure 6). The B.E. of this band is approximately the same for $\underline{PrNH_2}$ and en-silanized surfaces, and on RuO_2 and TiO_2, where accurate B.E. measurements were feasible. The intensity of the higher B.E. band roughly correlates with the intensity of the N 1s band of the alkylaminesilane and thus it is related to coverage achieved in the silanization reaction. It is particularly intense on samples bearing siloxane polymer. The lattice O 1s band exhibits no change in B.E. upon silanization but is lowered in intensity presumably due to photoelectron scattering by the overlying silane.

The higher B.E. O 1s band which appears upon silanization can be interpreted as -MOSi- oxygen, (although contributions from -SiOH, -SiOR, or adsorbed water are also possibilities). The lattice O 1s band for -SiOSi- bound oxygen (as in silica) lies at higher B.E. (by 2-3 e.v., see data in Table III) than the typical lattice oxygen in the more ionic metal oxides. The band on silanized metal oxide has an intermediate B.E.; compare 530.0 e.v. for TiO_2 lattice O 1s and 532.5 e.v. for glass (our data) with the observed

532.0 e.v. on TiO_2/en. This would qualitatively be expected for -MOSi- oxygen. The -MOSi- band overlies or supplants by reaction the surface hydroxyl present on the metal oxide before silanization. In the case of SnO_2, care must be taken to avoid specimens with surface Si contaminant when examining the effects of silanization.

The O 1s spectral region has potential qualitative usefulness in study of silanization reactions. We regard quantitative interpretations of intensities as tenuous due to the metal hydroxyl feature and the presence of surface water, adsorption of which is conceivably enhanced by the presence of the silane.

SnO_2 Dopant Concentration and Depth Profile

SnO_2, an n-type semiconductor in pure form, is useful as a non-rectifying working electrode at positive potentials only when doped with high levels of appropriate carriers. The SnO_2 electrodes employed here are fluoride doped; a F 1s band can be detected for this at B.E. 687 e.v. The dopant concentration and depth profile are of interest. Figure 7 shows Ar^+ sputter profiles for two native SnO_2 and one silanized SnO_2 electrodes. The variation of I_F with sputter time indicates that the outermost 10-20 Å of the SnO_2 electrode is depleted in dopant. The degree of depletion varies with the electrode as does the interior level of dopant. There is no obvious dependence on the electrode having been subjected to silanization. Applying equation 1 in the same manner as for N/Si, a relative sensitivity factor of 0.26 is used to convert the I_F/I_{Sn} band area ratios (Figure inset) for Specimen II at zero sputtering time (surface) and 10 minutes sputtering time (interior) to F/Sn atom ratios of 0.034 and 0.056, respectively. These are approximate values since I_F for Specimen I, for instance, was twice as large, and also the

relative sensitivity factor was not compared to standards. Using 6.95 g.cm.^{3} for SnO_2 density, carrier populations of 9.4×10^{20} and 1.6×10^{21} atoms/cm^3 are calculated for the SnO_2 surface and bulk, respectively. The surface carrier population is sufficiently high that adverse electrochemical properties are not expected from the depletion effect, and importantly the depletion effect is not enhanced by the silanization reaction.

The dopant depletion for SnO_2 is in contrast to Sn-doped In_2O_3, which according to Kuwana exhibits a higher Sn/In ratio at the surface of this electrode material than in its bulk (57).

Figure 7 also shows a variation of I_O/I_{Sn} (band areas) with Ar^+ sputtering similar to a previous measurement (57). The F dopant depletion falls within the region of enhanced I_O/I_{Sn}, which we interpret as a layer of partially hydrated SnO_2 lattice, for the following reasons. Using a relative O/Sn sensitivity factor 0.20 derived from equation 1, the calculated O/Sn atom ratio for SnO_2 electrodes varies typically from 2.4 prior to sputtering to about 1.4 after sputtering attains a constant I_O/I_{Sn}. (One sample gave an initial O/Sn ratio of 3.5, but the same final value.) These calculations, by themselves, suggest that while the outermost surface is hydrated, the Ar^+ beam sputtering induces a chemical change in the SnO_2 to a lower oxide form and so the actual depth of lattice hydration is less than the profile of Figure 7 implies. The possibility of reduction during sputtering of SnO_2 powder has been advanced (47). In an alternate interpretation, using an emperical relative O/Sn sensitivity factor 0.11 (58) with Figure 7 yields O/Sn atom ratios typically 4.3 before sputtering and 2.5 after. This calculation suggests even more extensive surface hydration and little or no Ar^+ reduction effect. A sputtering experiment with 400 e.v. Ar^+ was stated elsewhere not to cause reduction of SnO_2 (59). Lastly, we have observed an example of metal ion chemisorption (60)

to the same depths as the I_O/I_{Sn} variation , The evidence supports our interpretation of Figure 7 in terms of a hydration deeper than the outermost SnO_2 lattice plane.

DISCUSSION

For the most part, the above results show that the alkylaminesilanized surfaces exhibit expected and understandable properties, and the hope of chemical amine-like predictability of the modified metal oxide electrode surface is qualitatively realized. The alkylaminesilanized interface cannot, on the other hand, be considered as solely an amine-like surface; its chemistry is more complex than this. This is not surprising for a surface synthesized under conditions far from the atomically clean single crystal domain. Such chemical complexity will probably be common for other forms of electrode surface modification upon examination on a comparable level of detail.

The motivation for our study of the alkylaminesilanized interface is in its use as a connecting bridge for immobilization of redox reagents on electrode surfaces. We should consider how the present results relate to that application. The alkylaminesilane chain is not itself a good electron transport bridge between immobilized redox reagent and electrode. The length of a bonded en silane from metal to primary amine nitrogen is ∿12 Å in extended form and ∿9 Å in the hydrogen bonded Structure VII. Unless the activation barrier for electron transfer over such distance proves to be modest, flexible motions of the alkylaminesilane chain will play a role in the electron transfer process. The premise of the so-called "floppy model" (2, 24) is that such flexibility will exist in these modified surfaces. At least three factors are involved, the frequency of the motion, which will influence the pre-exponential kinetic factor (maximum value $kT/h \sim 10^{13}$ sec^{-1}) (61, 62), and the distance and geometry of redox reagent approach to metal

oxide, which will influence $\Delta G^{\ddagger}$. Motions of the alkylaminesilane chain will be affected by Structures I-III, V, VI, and VII. Overall stability of the modified surface is enhanced by multiple -MOSi- bonds, and by cross-linking as in Structure V, but motional freedom of the amine site diminishes in the order of Structures I > II > III. We conjectured that I and II are more likely, but no quantitative analysis of this bonding problem is available. Structures VI and VII provide a shorter connecting bridge but also tend to restrain the approach distance. It would appear from the amidization data that the hydrogen-bonded structures may be prevalent in alkylaminesilanes with γ-amine sites. For purposes of modeling of electron-transfer events, then, combinations of Structures I and II with VI and VII probably present a good estimate of the average surface stereochemistry. A considerable complication in such modeling, however, is the possibility that very rapid electron transfer is to but a small population of sites possessing optimum alkylaminesilane chain flexibility. Subsequent lateral propagation of electron transfer to other more motionally restricted sites then might actually be the controlling mechanism. Quantitative modeling is tenuous until such eventualities are evaluated.

Our interpretation of the ESCA results indicates that a variety of surface structures may exist within a single specimen of alkylaminesilanized metal oxide electrode. We can draw from this the intimation that a redox reagent bound to the alkylaminesilane may find itself in a spectrum of slightly different chemical environments. The redox reagent may as a consequence exhibit a spectrum of formal electrochemical potentials, which in turn has the effect of broadening the electrochemical surface wave observed for the reagent. To what extent broadening we have observed in surface waves on alkylaminesilanized electrodes is due to this chemical heterogeneity as opposed

to interactive effects within the chemically bound layer (62) or to both, remains to be resolved.

Acknowledgement

Assistance from D. N. Smith in ESCA bandfitting is gratefully acknowledged.

Credit

This research was assisted by the National Science Foundation under grants MPS75-07863, CHE76-24564, DMR72-03024 and by the Office of Naval Research.

References

1. P. R. Moses, L. Wier and R. W. Murray, Anal. Chem., 47, 1882 (1975).

2. P. R. Moses and R. W. Murray, J. Electroanal. Chem., 77, 393 (1977).

3. J. R. Lenhard and R. W. Murray, Ibid., 78, 195 (1977).

3a. A. Diaz, J. Amer. Chem. Soc., 99, 5838 (1977).

3b. G. J. Leigh and C. J. Pickett, J. Chem. Soc., Dalton, Ed., 1797 (1977).

4. C. M. Elliott and R. W. Murray, Anal. Chem., 48, 1247 (1976).

5. P. R. Moses, J. C. Lennox, J. Lenhard and R. W. Murray, 173rd Amer. Chem. Soc. Meeting, New Orleans, La., March 1977.

6. D. F. Untereker, J. C. Lennox, L. M. Wier, P. R. Moses and R. W. Murray, J. Electroanal. Chem., 81, 309 (1977).

7. M. Fujihira, T. Matsue and T. Osa, Chem. Lett. (Japan) 875 (1976).

8. D. F. Untereker, P. R. Moses, L. M. Wier, C. M. Elliott and R. W. Murray, 149th Electrochem. Soc. Meeting, Washington, D.C., May 1976.

9. E. Grushka, ed., Bonded Stationary Phases in Chromatography, Ann Arbor Science Publications, Ann Arbor, Mich., 1974.

10. C. H. Lochmuller and C. W. Amoss, J. Chromatogr., 108, 85 (1975).

11. E. Grushka and E. J. Kikta, Jr., Anal. Chem., 46, 1370 (1974).

12. H. H. Weetall, Sep. and Purif. Methods, 2, 199 (1973).

13. D. M. Hercules, L. E. Cox, S. Onisick, G. D. Nichols and J. C. Carver, Anal. Chem., 45, 1973 (1973).

14. D. E. Leyden and G. H. Luttrell, Anal. Chem., 47, 1612 (1975).

15. R. L. Burwell, Chem. Technol., 370 (1974).

16. E. P. Pluddemann, Adhesion Age, 18, 36 (1975); Chem. Abstr., 83, 148735 (1975).

17. K. Hardee and A. J. Bard, J. Electrochem. Soc., 122, 739 (1975).

18. C. N. Reilley and W. S. Woodward, to be submitted for publication.

19. H. P. Boehm, "Chemical Identification of Surface Groups," Advances in Catalysis, 16, 179 (1966).

20. R. K. Gilpin and M. F. Burke, Anal. Chem., 45, 1383 (1973).

21. E. W. Thornton and P. G. Harrison, J. Chem. Soc. Faraday Trans. I, 71, 461 (1975).

22. D. J. C. Yates, J. Phys. Chem., 65, 746 (1961).

23. H. Kuhn, "Spectroscopy of Monolayer Assemblies," in Physical Methods of Chemistry, A. Weissberger and B. Rossiter, eds., Part IIIB, p. 577, Wiley, 1972.

24. P. R. Moses and R. W. Murray, J. Amer. Chem. Soc., 98, 1435 (1976).

25. M. Gleria and R. Memming, Z. Physik. Chem. Neve Folge, 98, 303 (1975).

26. A. A. Oswald, L. L. Murrel and L. J. Boucher, Abstr. Div. Petroleum Chem., 168th National American Chemical Society Meeting, Los Angeles, Calif., 1974.

27. P. G. Harrison and E. W. Thornton, J. Chem. Soc. Faraday Trans. I, 1310 (1976).

28. A. Diaz, J. Amer. Chem. Soc., 99, 6780 (1977).

29. V. S. Srinivasan and W. J. Lamb, Anal. Chem., 49, 1639 (1977).

30. J. H. Scofield, Lawrence Livermore Laboratory Report No. UCRL-51326, January, 1973.

31. D. M. Hercules, Anal. Chem., 42, 20A(1) (1970).

32. S. Pignataro and G. Distefano, J. Electron Spectrosc. Rel. Phenom., 2, 171 (1973).

33. H. F. Weetall and L. S. Hersh, Biochim. Biophys. Acta, 206, 54 (1970).

34. L. Lee, J. Colloid Interfac. Sci., 27, 751 (1968).

35. E. P. Plueddeman, J. Adhesion, 2, 184 (1970).

36. M. L. Hair, Infrared Spectroscopy in Surface Chemistry, M. Dekker, N.Y., 1967, p. 102.

37. F. J. Kahn, Appl. Phys. Letts., 22, 386 (1973).

38. H. R. Anderson, F. M. Fowkes and F. H. Hielscher, J. Polym. Sci., Polym. Phys. Ed., 14, 879 (1976).

39. J. C. Lennox and R. W. Murray, J. Electroanal. Chem., 78, 195 (1977).

40. J. N. Butler, Ionic Equilibria, Addison Wesley, Reading, Mass., 1964, p. 466.

41. R. F. Reilman, A. Msezane and S. T. Manson, J. Electron Spectrosc. Rel. Phenom., 8, 389 (1976).

42. C. D. Wagner, Anal. Chem., 49, 1282 (1977).

43. D. R. Penn, J. Electron Spectrosc. Rel. Phenom., 9, 29 (1976).

44. J. C. Helmer and N. H. Weichert, Appl. Phys. Lett., 13, 266 (1968).

45. J. S. Johannessen, W. E. Spicer and Y. E. Strausser, Thin Solid Films, 32, 311 (1976).

46. P. H. Holloway and H. J. Stein, J. Electrochem. Soc., 123, 723 (1976).

47. A. W. C. Lin, N. R. Armstrong and T. Kuwana, private communication, 3/77.

48. K. S. Kim and N. Winograd, J. Catalysis, 35, 66 (1974).

49. N. S. McIntyre and M. G. Cook, Anal. Chem., 47, 2208 (1975).

50. W. Dianis and J. E. Lester, Surface Science, 43, 602 (1974).

51. T. Robert, M. Bartel and G. Offergeld, Surface Science, 33, 123 (1972).

52. K. S. Kim, A. F. Gossmann and N. Winograd, Anal. Chem., 46, 197 (1974).

53. G. C. Allen, M. T. Curtis, A. J. Hooper and P. M. Tucker, J. Chem. Soc., Dalton Trans., 1525 (1974).

54. K. Kishi and S. Ikeda, Bull. Chem. Soc. Japan, 46, 341 (1973).

55. J. P. Rynd and A. K. Rastogi, Surface Science, 48, 22 (1975).

56. S. R. Nagel, J. Tauc and B. G. Bagley, Solid State Commun., 20, 245 (1976).

57. N. R. Armstrong, A. W. C. Lin, M. Fujihira and T. Kuwana, Anal. Chem., 48, 741 (1976).

58. C. D. Wagner, Anal. Chem., 44, 1050 (1972).

59. K. S. Kim, W. E. Baitinger, J. W. Amy and N. Winograd, J. Electron Spectrosc. Rel. Phenom., 5, 351 (1974).

60. L. Wier, unpublished results, U.N.C., 1976.

61. R. C. Baetzoldanel and G. A. Somorjai, J. Catalysis, 45, 94 (1976).

62. F. C. Anson, U.S.-Japan Seminar, San Francisco, Calif., May, 1977.

Table I

Assay of Active Amine

Acid Base Assay

Expt	Electrode[a]	Treatment[b]	$I_{N\ 1s(400)}/I_{N\ 1s(401.5)}$[c]	Active Amine[d]
I-1	$SnO_2/PrNH_2$	pH 10 wash	76/24%	
		0.05 M HCl wash	58/42	16%
I-2	SnO_2/en	pH 10 wash	72/28	
		0.05 M HCl wash	41/59	31%
I-3	RuO_2/en	pH 10 wash	61/37	
		0.05 M HCl wash	39/63	26%

Amidization Assay

Expt	Electrode[a]	Treatment[b]	$\frac{I_{N\ 1s(406.5)}}{I_{N\ 1s(Amine+Amide)}}$	$\frac{I_{F\ 1s(687)}}{I_{N\ 1s(Amine+Amide)}}$	Active Amine[d]
I-4	$SnO_2/PrNH_2$	4-(NO_2)ØCOCl	0.20[f],0.27		20%[f],27%
I-5	$SnO_2/PrNH_2$	3,5-$(NO_2)_2$ØCOCl	0.13		6%
I-6	$SnO_2/PrNH_2$	4-FØCOCl		0.53	22%
I-7	SnO_2/en	4-(NO_2)ØCOCl	0.29		29%
I-8	SnO_2/en	3,5-$(NO_2)_2$ØCOCl	0.96[g],0.98,1.00		48,49,50%
I-9	SnO_2/en	4-FØCOCl		1.84	77%
I-10	$RuO_2/PrNH_2$[j]	3,5-$(NO_2)_2$COOH[i]	1.48		74%
I-11	$RuO_2/PrNH_2$[h]	3,5-$(NO_2)_2$COCl	0.42,0.27,0.33,0.30		21,13,16,15%
I-11a	$RuO_2/PrNH_2$[k]	4-(NO_2)ØCOCl	0.20		20%
I-12	RuO_2/en[h]	3,5-$(NO_2)_2$COCl	0.49,0.53,0.72,1.35		24,25,36,63%
I-13	TiO_2/en	3,5-$(NO_2)_2$COOH[i]	0.24		12%
I-13a	TiO_2/en	3-(NO_2)ØCH$_2$COOH[i]	0.21		21%
I-14	Pt/PtO/en	3,5-$(NO_2)_2$COCl	0.45		(23%)[l]
I-15	Pt/PtO/en	3,5-$(NO_2)_2$COOH[i]	0.45,0.68		(23,34%)[l]

Table I continued

a. Electrode/$\underline{PrNH_2}$ and electrode/$\underline{en}$ denote surfaces reacted using Method C with 3-aminopropyltriethoxysilane and 3-(2-aminoethylamino)propyltrimethoxysilane, respectively.

b. ESCA data comparing acid and base treatment are on separate specimens to avoid possible beam damage effects.

c. Intensities are in % of total amine band area; actual B.E. in alkylaminesilane doublet are 399.3 e.v. and 400.6 e.v. for $\underline{en}$ and 400.3 e.v. and 401.9 e.v. for $\underline{PrNH_2}$.

d. Percentage of total nitrogen intensity shifted to higher B.E. by acid wash.

e. Percentage of total alkylaminesilane N 1s band (Amine+Amide) which yields tagged derivative. Nitro derivatives normalized according to number of nitro sites; fluoro derivative normalized with cross-section (30) ratio 0.42.

f. Data taken from figure in ref. 7, silanization reaction Method A.

g. Silanization Method D used.

h. Thermal curing post-silanization treatment.

i. Amidization using DCC coupling procedure.

j. Anhydrous post-silanization handling, reactions conducted in glove box.

k. Silanization Method E used.

l. See text.

Table II

N/Si Surface Atom Ratio From ESCA Band Intensities

Alkylaminesilanized Electrodes

Expt	Electrode	I_N/I_{Si}[a]	Calc N/Si[b]	N/Si in Silane[c]	Silane N/Si / Calc N/Si
II-1	SnO_2/en[d]	1.09±0.38(8)	0.60	2	3.33
II-2	SnO_2/en[e]				
	(10 sec)	2.95	1.62	2	1.23
	(20 sec)	2.42	1.33	2	1.50
	(1 min)	2.64	1.45	2	1.38
	(3 min)	1.29	0.71	2	2.82
	(6 min)	1.33	0.73	2	2.74
II-3	SnO_2/en[f]	1.34	0.74	2	2.70
II-4	SnO_2/en[g]	1.93	1.06	2	1.89
II-5	$RuO_2/PrNH_2$[h]	1.46±0.10(4)	0.80	1	1.25
II-6	RuO_2/PrNH [i]	1.76±0.09(4)	0.97	1	1.03
II-7	RuO_2/en[h]	2.52±0.36(2)	1.38	2	1.45
II-8	RuO_2/en[i]	2.86	1.57	2	1.27
II-9	RuO_2/triam[h]	5.77	3.17	3	0.95
II-10	TiO_2/en[h]	3.42±0.38(3)	1.88	2	1.06
II-11	Pt/PtO/en[h]	7.0±1.0(6)	4.02	2	0.50
II-12	Pt/PtO/en[i]	2.70±0.22(2)[j]	1.55	2	1.29

Standard Materials

Expt	Sample	I_N/I_{Si}	Calc N/Si[b]	Actual N/Si	Actual/Calc
II-13	Si_3N_4	1.74±0.16(3)	0.96	1.33	1.39
II-14	$PrNH_2$ silane polymer[k]	1.85	1.02	0.91[l]	0.89
II-15	en silane polymer[k]	2.78	1.53	1.54[l]	1.01
II-16	triam silane polymer[k]	4.55	2.50	3.05[l]	1.22

a. Band area ratios of N 1s at 401.5+400 e.v. to Si 2p at 102 e.v., except for Expts II-11, 12, which used Si 2s at 160 e.v. to avoid interference with a Pt band. Number of specimens in ( ).

b. Band area ratio converted to atom ratio using sensitivity factor of N/Si of 1.82 to N 1s/Si 2p and 1.74 for N 1s/Si 2s. See text.

c. Stoichiometric atom ratio in the indicated pure silane.

d. Electrodes prepared using silanization Method A.

Table II continued

e. Silanization Method D; data from Figure 1.

f. Silanization Method D.

g. Silanization Method D followed by amidization with 4-(NO_2)ØCOCl.

h. Silanization Method C.

i. Silanization Method C followed by amidization with 3,5-(NO_2)$_2$ØCOOH (DCC).

j. Band area ratio of N 1s at 406 e.v. to Si 2s at 160 e.v. and assumption of 50% active amine.

k. Polymer samples prepared from silane by hydrolysis with water, drying, grinding to powder.

l. Polymer sample analysis by Galbraith Laboratories.

Table III

O 1s Binding Energies

Sample	O 1s B.E., e.v.[a]			Source
			lattice	
SnO_2	sh	,	530.8	this work
	532(sh)	,	530.5	(7)
	531.7[b]	,	530.1	(47)
$SnO_2/PrNH_2$	531.8	,	sh	this work
SnO_2/en	∿531.5	,	530.8	this work
$SnO_2/PrNH_2$	532	,	530.5(sh)	(7)
RuO_2	∿532	,	529.6	this work
RuO_2	530.5(sh)[c]	,	529.4	(48)
$RuO_2/PrNH_2$ (or en)	532.1±0.2	,	529.7±0.2	this work
TiO_2	sh	,	530.0	this work
TiO_2/en	532.0±0.3	,	529.8±0.3	this work
porous silica			532.8	this work
glass			532.5	this work
glass fibers			532.4	(55)
glass			531.2,529.4[d]	(56)
NiO	531.2[b]		529.4	(50)
CuO	531.6[b]		529.7	(51)

a. B.E. in this work referenced to C 1s (285 e.v.); B.E. by others referenced variously to Au, Ag, C 1s, and exact correspondence B.E. cannot be expected.

b. Interpreted variously as chemisorbed oxygen species or surface hydroxyl.

c. Hydrated sample; pure prepared sample has 531.5 band interpreted as RuO_3 defect.

d. Interpreted as "non-bridging oxygen."

Figure Legends

Figure 1 Reaction kinetics of en silane in 6°C benzene with SnO_2. Reaction quenched with benzene rinse. (———) $I_{N\ 1s}$ for 1% silane solution, (—□—) $I_{N\ 1s}$ for 0.1% solution, (—○—) for 0.001% solution; (—X—) $I_{Si\ 2p}$ for 1% solution. N 1s spectral inset for data point "A."

Figure 2 1.5 Kev Ar^+ sputter of SnO_2/en electrodes prepared by Method D (———) and by a Method A experiment in which polymer formed (-----).

Figure 3 Cyclic voltammograms on SnO_2 (Curves A, D), SnO_2/en prepared with Method D (Curves B, E), and SnO_2/en prepared with Method A (Curves C, F). Same electrode preparation as used for data of Figure 2 but different specimens. Curves A-C: ca. 2 mM ferrocyanide in 0.1 M KCl and pH 2.4, 0.5 M glycine buffer. 200 mv/sec. Curves D-F: 1 mM $Ru(bpy)_3(ClO_4)_2$ in 0.18 M H_2SO_4, 0.1 M KCl. 200 mv/sec.

Figure 4 N 1s spectra for SnO_2/$PrNH_2$ (Curves A, B) and SnO_2/en (Curves C, D) electrodes exposed to pH 10 aqueous base (lower) and to 0.05 M HCl (upper) resolved into protonated and free base spectral components. Different samples used for each experiment.

Figure 5 Ratio of protonated and free base (I_{NH}/I_N) N 1s intensities on glassy carbon/en electrodes as a function of pH of aqueous buffer to which the surface was exposed. Inset shows resolving of two N 1s components. Different sample used for each pH point.

Figure 6 O 1s spectra on various metal oxides. Curve A: RuO_2; Curve B: RuO_2/en; Curve C: RuO_2/$PrNH_2$; Curve D: SnO_2; Curve E: SnO_2/$PrNH_2$; Curve F: TiO_2; Curve G: TiO_2/en.

Figure 7 1.5 Kev Ar^+ sputter profile for SnO_2 (Specimen I, -●-, and specimen II, -O-) and SnO_2/en (Method D, Specimen III, -Δ-) electrodes for O 1s, Sn $3d_{5/2}$, and F 1s. Sputter profiles are on arbitrary intensity scales different for each element; band intensity ratios in inset are actual band areas.

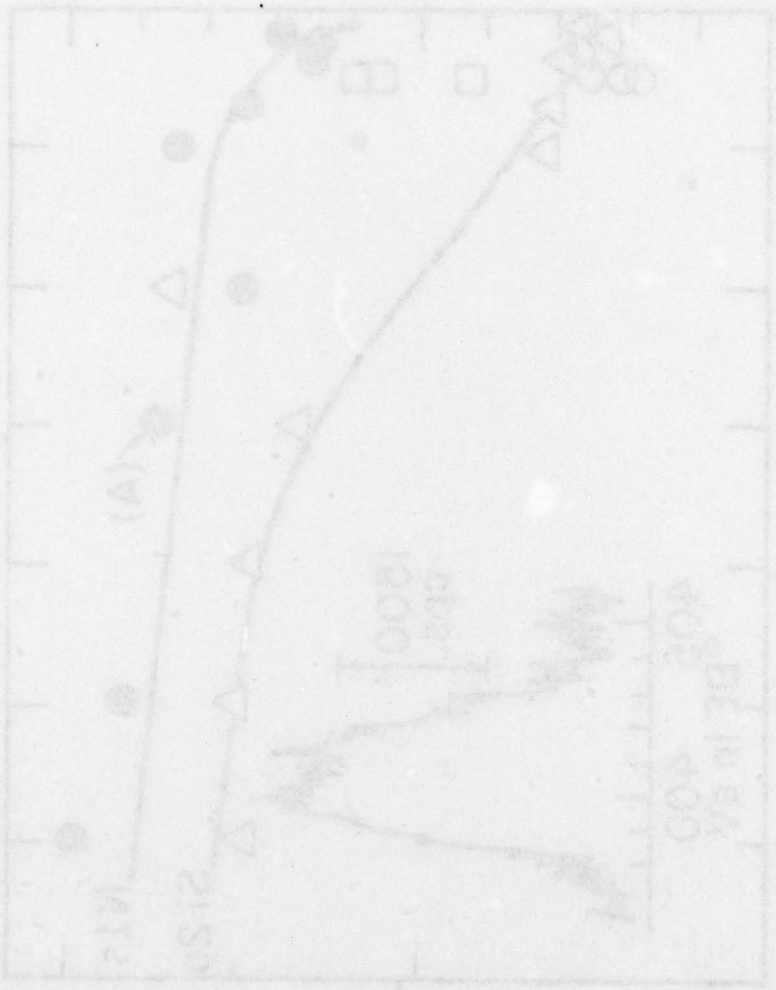

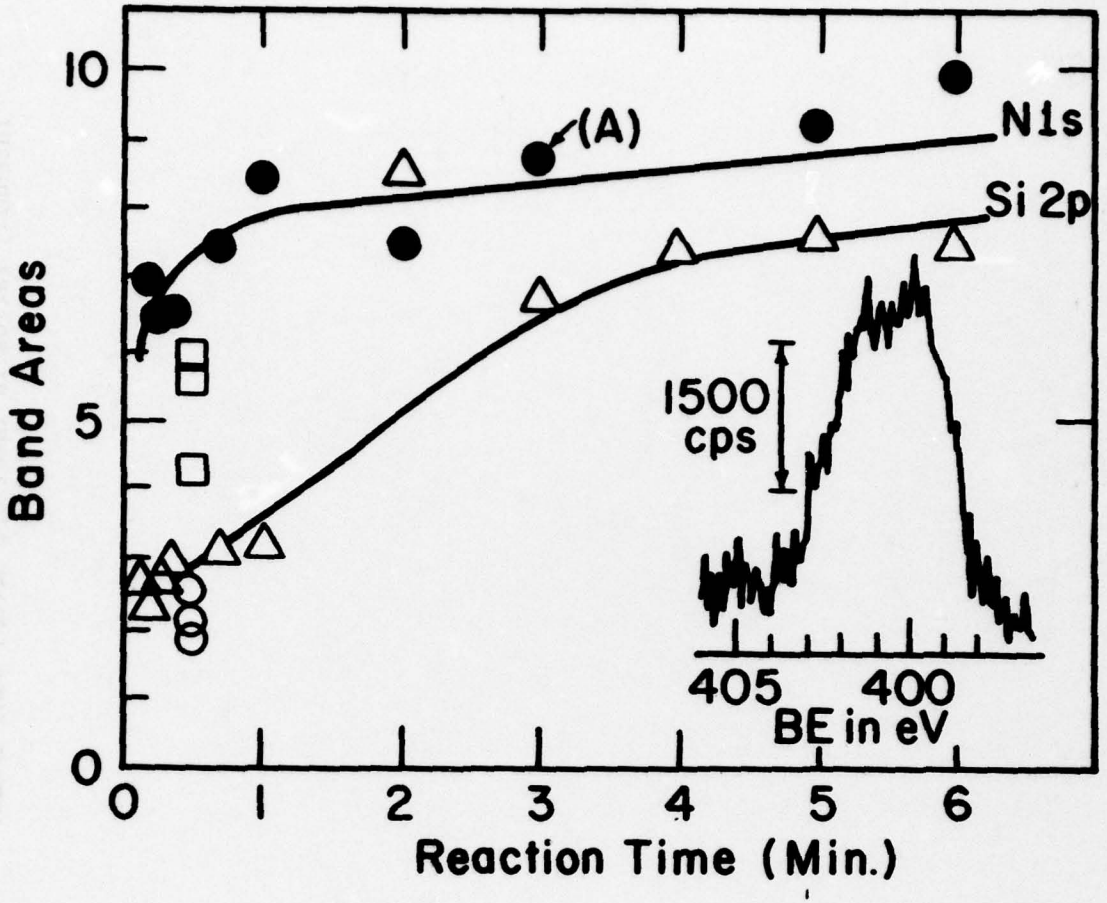
10
5
0
Band Areas
(A)
N1s
Si 2p
1500
cps
405
400
BE in eV
0
1
2
3
4
5
6
Reaction Time (Min.)

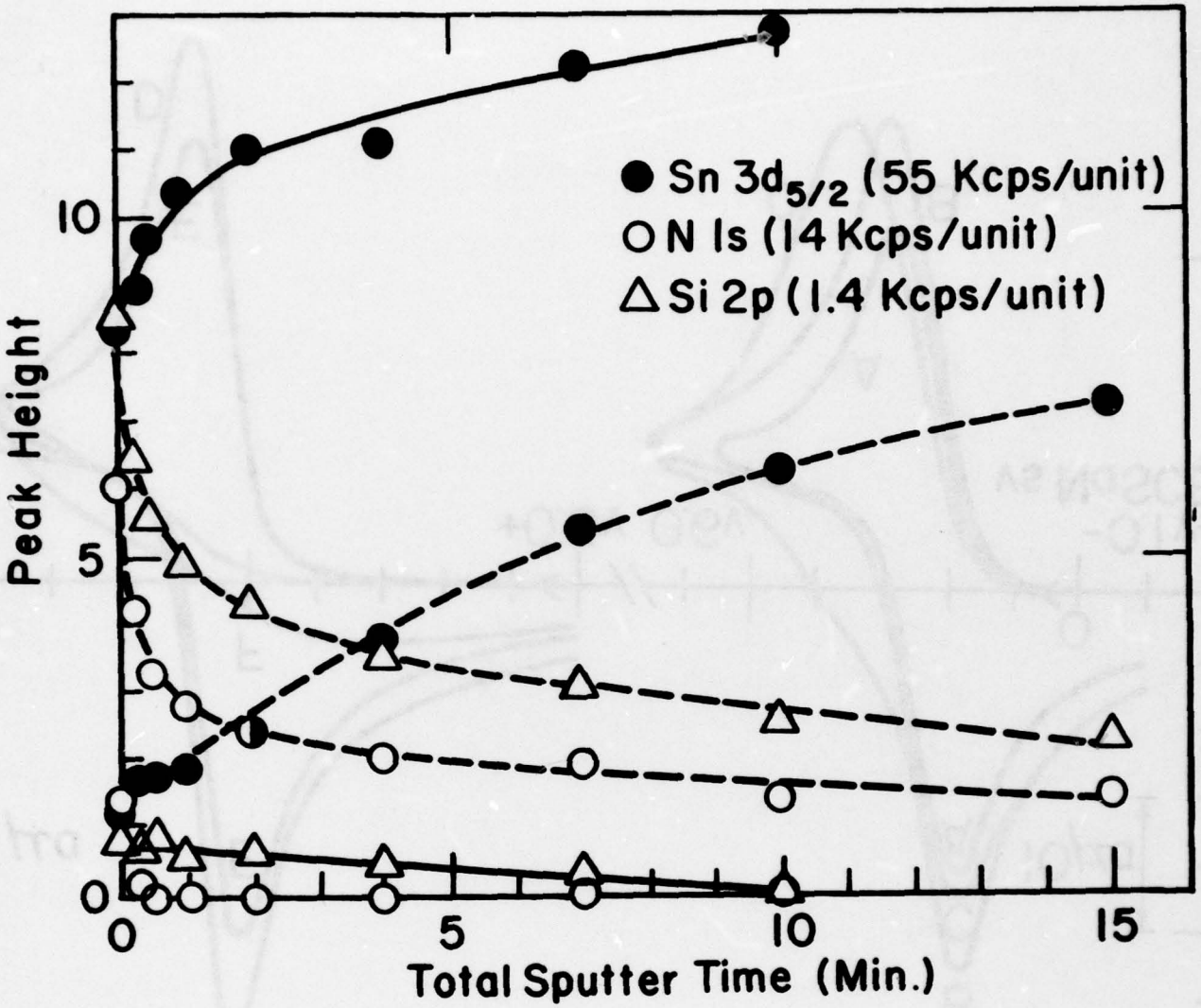
● Sn 3d5/2 (55 Kcps/unit)
○ N Is (14 Kcps/unit)
△ Si 2p (1.4 Kcps/unit)
Peak Height
0
5
10
0
5
10
15
Total Sputter Time (Min.)

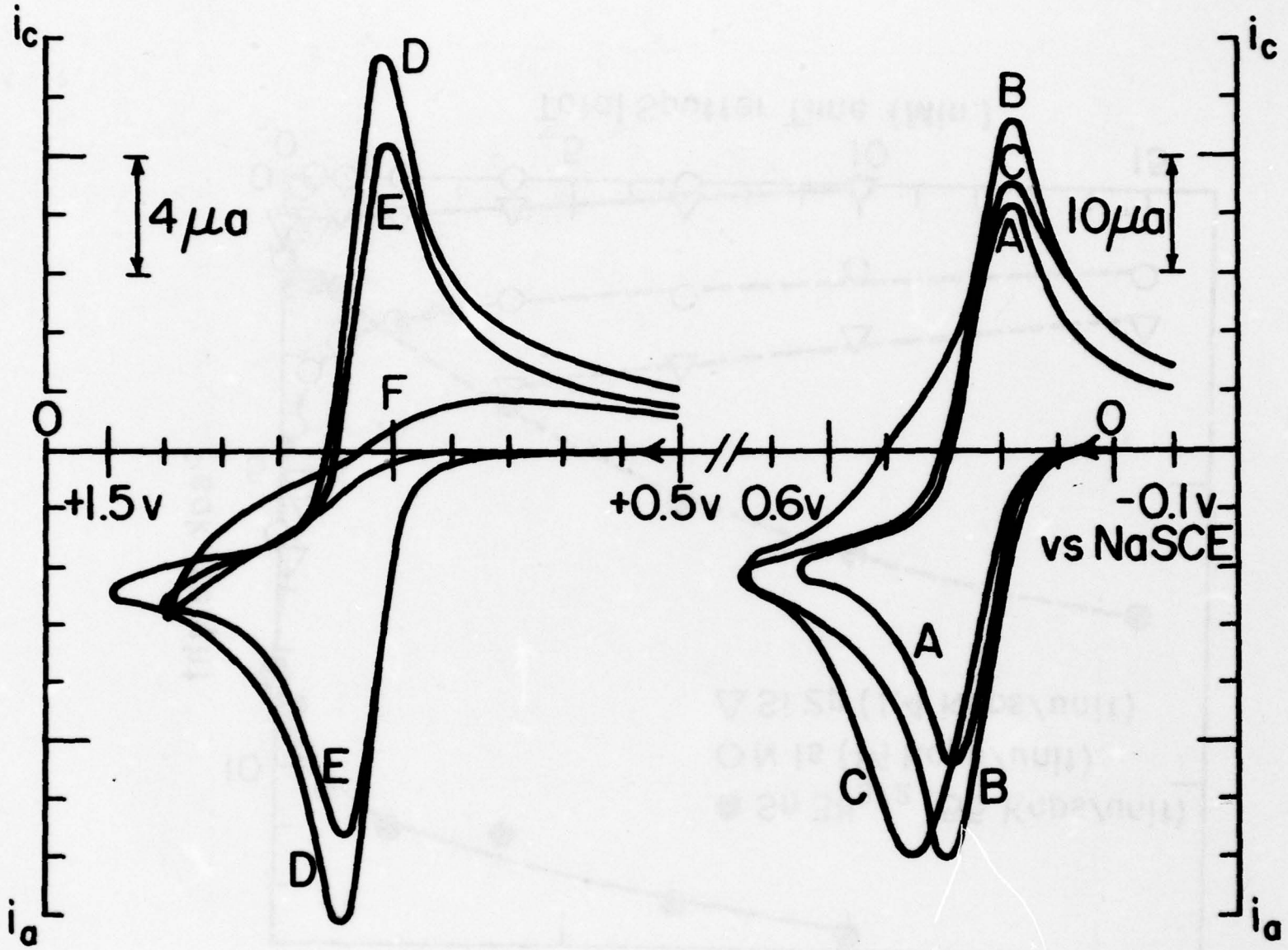
i_c
D
E
F
4μa
O
+1.5v
+0.5v
i_a
E
D
B
C
A
10μa
O
0.6v
-0.1v
vs NaSCE
A
C
B
i_c
i_a

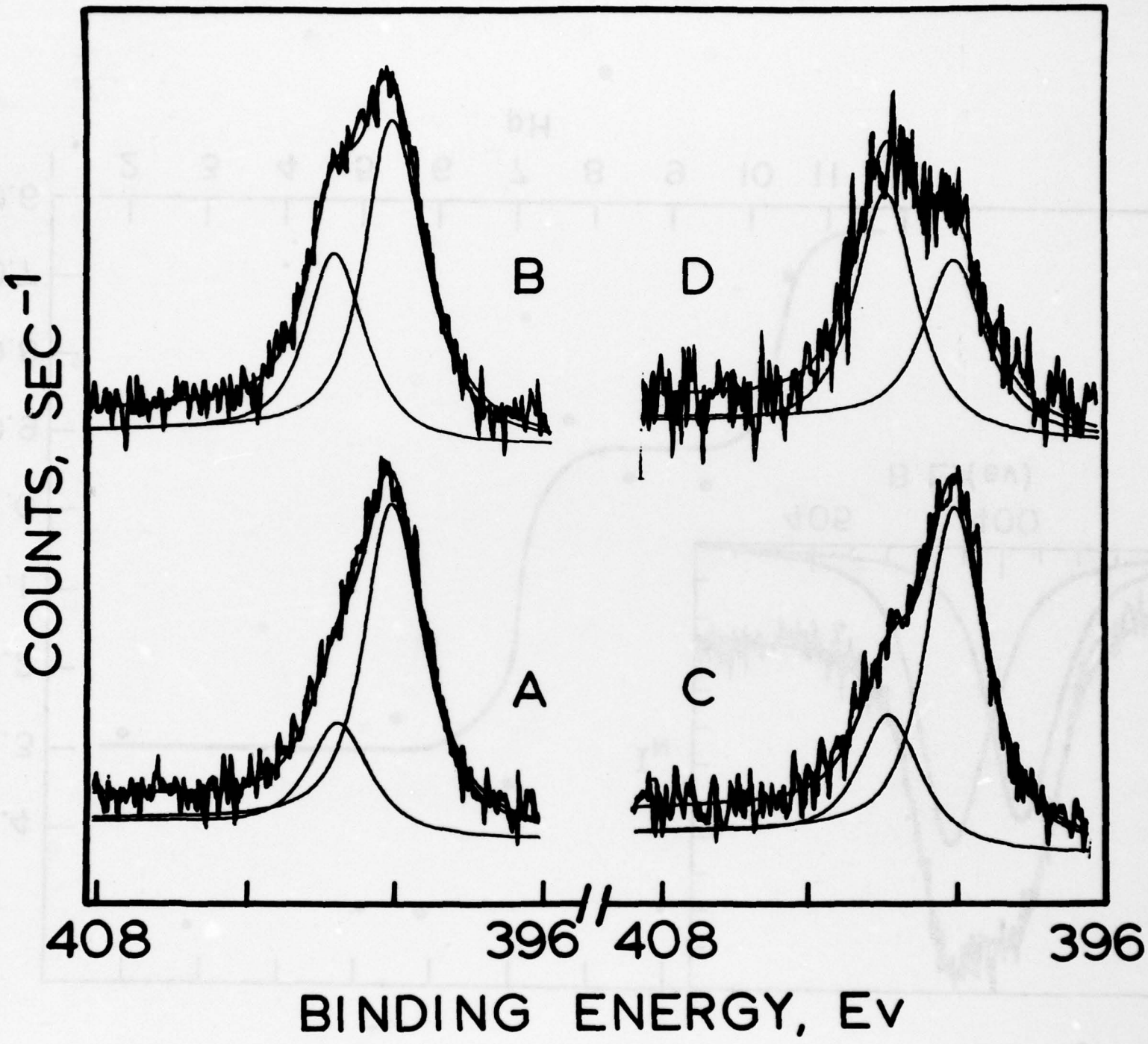
COUNTS, SEC⁻¹
B
D
A
C
408
396
408
396
BINDING ENERGY, Ev

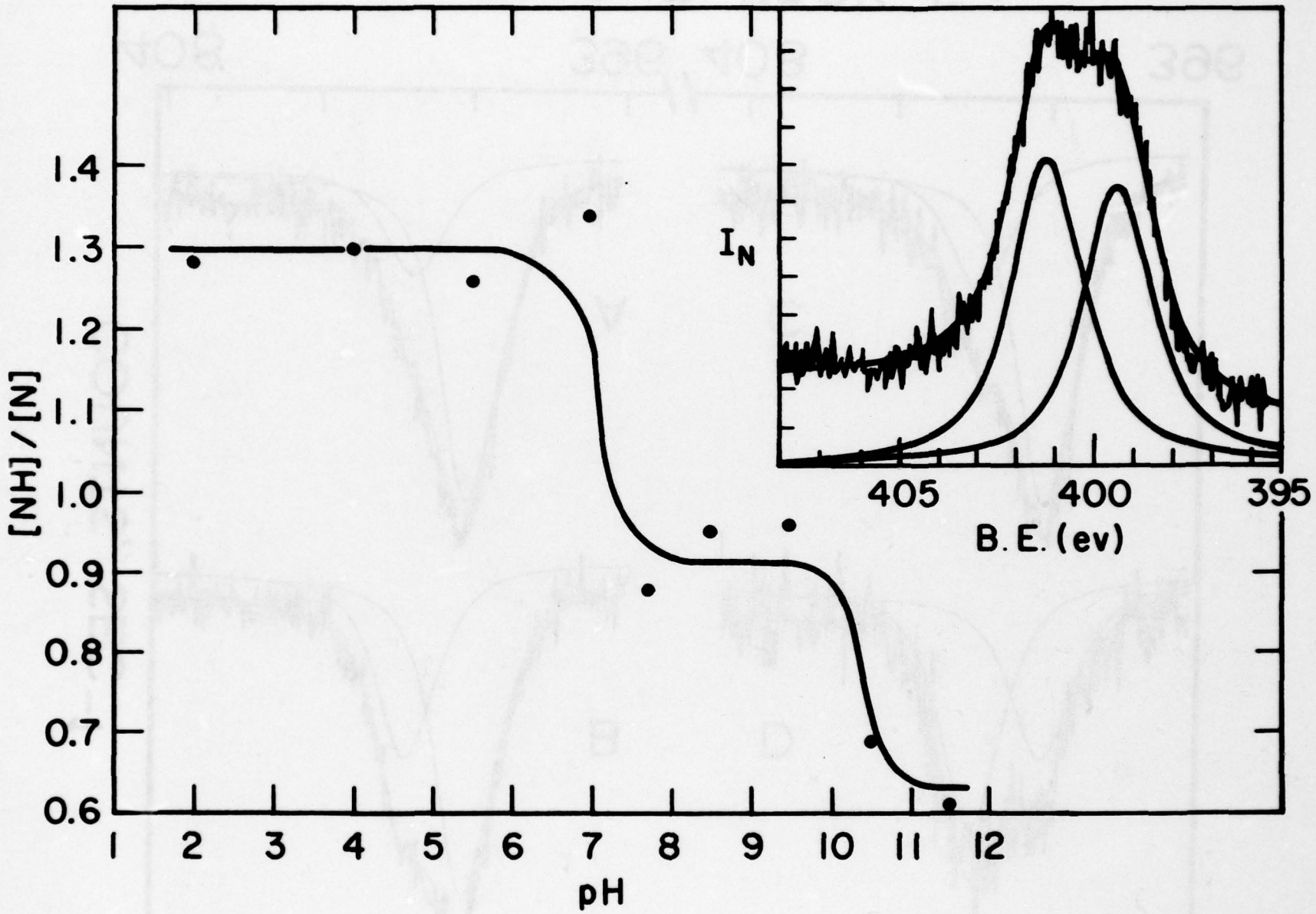
1.4
1.3
1.2
1.1
1.0
0.9
0.8
0.7
0.6
[NH] / [N]
1
2
3
4
5
6
7
8
9
10
11
12
pH
I_N
405
400
395
B. E. (ev)

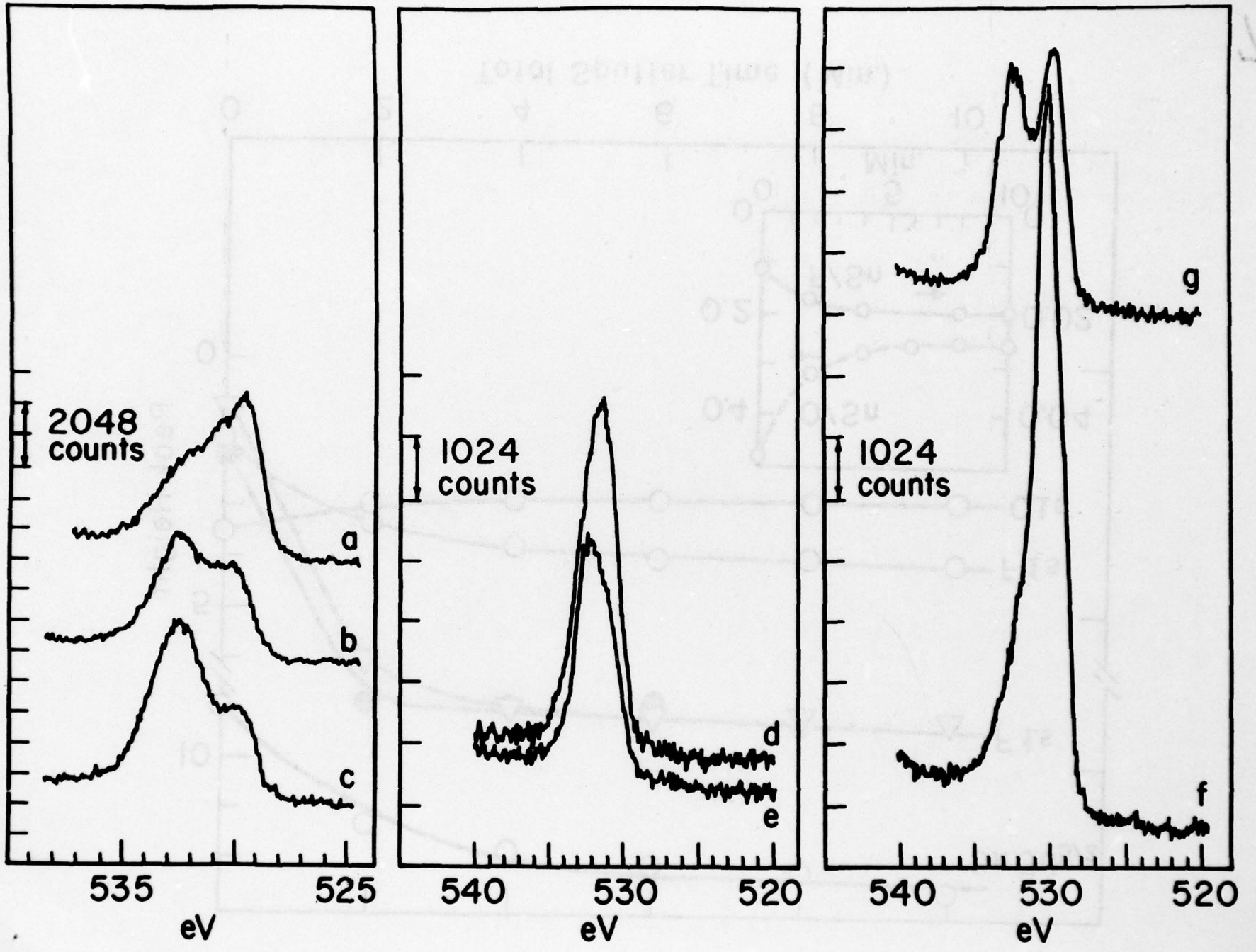
2048
counts
a
b
c
535
525
eV
1024
counts
d
e
540
530
520
eV
1024
counts
g
f
540
530
520
eV

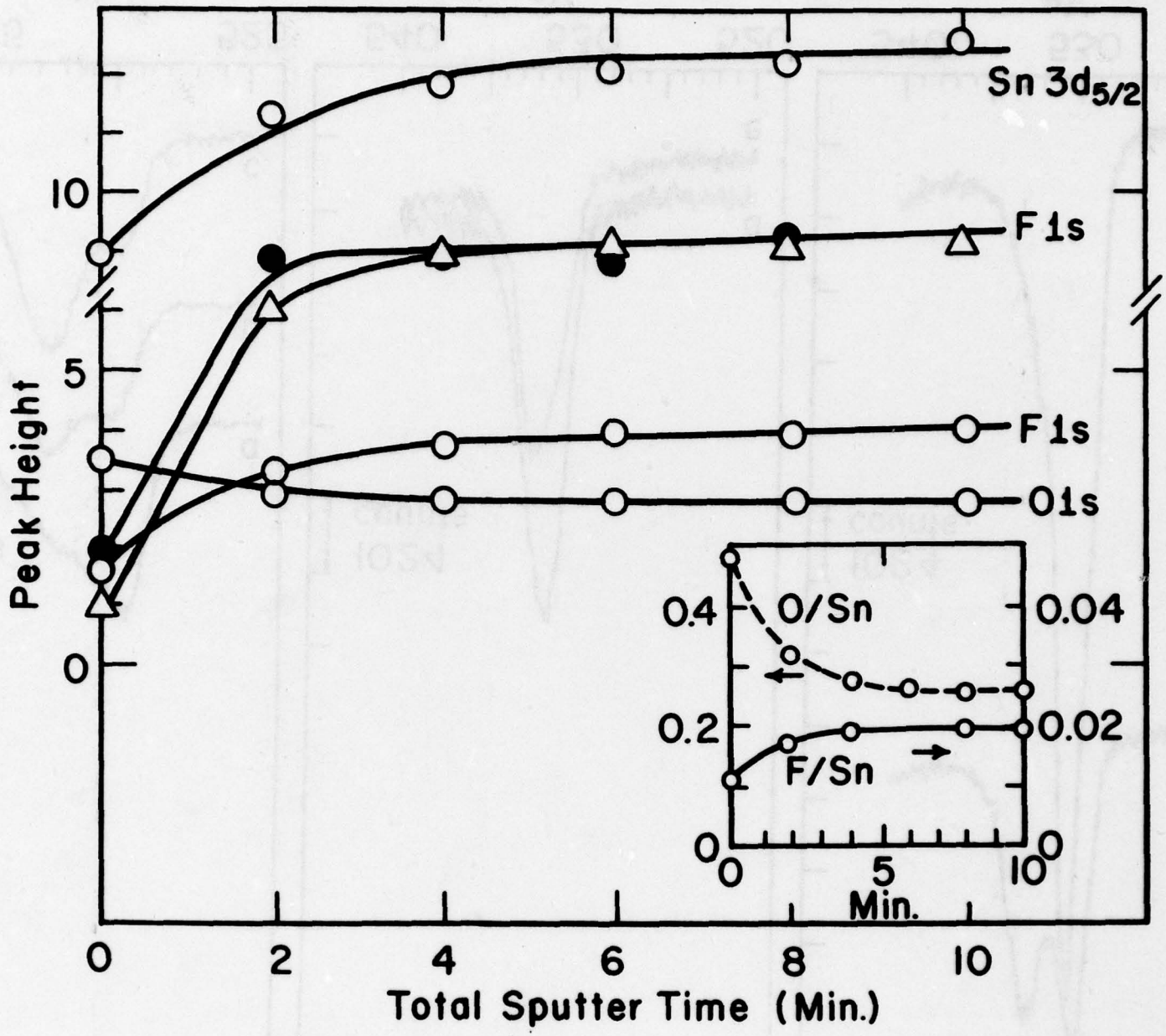
Sn 3d5/2
F 1s
F 1s
O 1s
Peak Height
10
5
0
0
2
4
6
8
10
Total Sputter Time (Min.)
0.4
0.2
0
O/Sn
F/Sn
0.04
0.02
0
0
5
10
Min.